Article

A Novel Hybrid Sine Cosine Algorithm and Pattern Search for Optimal Coordination of Power System Damping Controllers

Mahdiyeh Eslami [1,*] , Mehdi Neshat [2] and Saifulnizam Abd. Khalid [3]
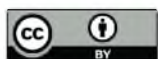
1 Department of Electrical Engineering, Kerman Branch, Islamic Azad University, Kerman 7635131167, Iran
2 Centre for Artificial Intelligence Research and Optimization, Torrens University Australia, Brisbane, QLD 4006, Australia; neshat.mehdi@torrens.edu.au
3 School of Electrical Engineering, Faculty of Engineering, Universiti Teknologi Malaysia, Johor Bahru 81310, Malaysia; saifulnizam@utm.my
* Correspondence: m.eslami@iauk.ac.ir

Abstract: This paper presents an effective hybrid optimization technique based on a chaotic sine cosine algorithm (CSCA) and pattern search (PS) for the coordinated design of power system stabilizers (PSSs) and static VAR compensator (SVC)-based controllers. For this purpose, the design problem is considered as an optimization problem whose decision variables are the controllers' parameters. Due to the nonlinearities of large, interconnected power systems, methods capable of handling any nonlinearity of power networks are preferable. In this regard, a nonlinear time domain-based objective function was used. Then, the proposed hybrid chaotic sine cosine pattern search (hCSC-PS) algorithm was employed for solving this optimization problem. The proposed method employed the global search ability of SCA and the local search ability of PS. The performance of the new hCSC-PS was investigated using a set of benchmark functions, and then the results were compared with those of the standard SCA and some other methods from the literature. In addition, a case study from the literature is considered to evaluate the efficiency of the proposed hCSC-PS for the coordinated design of controllers in the power system. PSSs and additional SVC controllers are being considered to demonstrate the feasibility of the new technique. In order to ensure the robustness and performance of the proposed controller, the objective function is evaluated for various extreme loading conditions and system configurations. The numerical investigations show that the new approach may provide better optimal damping and outperforms previous methods. Nonlinear time-domain simulation shows the superiority of the proposed controller and its ability in providing efficient damping of electromechanical oscillations.

Keywords: sine cosine algorithm; pattern search; PSS; SVC; optimization; oscillation

1. Introduction

The stability of power systems has become a key study area as a result of the integration of power systems. As a result, the power system has been upgraded with more complex control technology and stronger protective mechanisms to improve stability. Electromechanical oscillations, which can be categorized into inter-area and local modes, are detected in the power system as a result of mechanical and electrical torque imbalances at the synchronous generator, which are induced by changes in the power system topology or loads [1]. The generator rotor shaft and power transfers are severely damaged when these low frequency oscillations (LFOs) are insufficiently damped. These oscillations have a significant impact on the dependability and security of a power supply. Power system stabilizers (PSSs) have long been used to increase power system stability and boost system damping of oscillation modes in order to combat these negative phenomena. These stabilizers are used to add damping torque to the generator rotor oscillations that are caused by the generator's speed, frequency, or power. However, power networks are nonlinear and complex, making the use

of nonlinear models instead of linear approximations more advisable to treat any nonlinearity in the tuning problem. Moreover, recent research has revealed that if only one PSS is tuned, the required damping level cannot be reached. Thus, it is advised to ensure coordination between the design processes of all PSSs. From the literature review, such as in [1], it is shown that PSSs regulators may fail sometimes to provide adequate damping torque for inter-area modes. Unfortunately, some weakness is encountered in the damping of inter-area oscillations, and other solutions need to be involved.

In recent years, power electronic-based flexible AC transmission systems (FACTS) controllers, which are based on power electronics, have been considered as efficient alternative solutions [2]. Generally, FACTS devices have been employed for handling different power system control problems [3]. In other words, they can increase power transfer capability, and improve power system stability and controllability. Thus, power flow will be better controlled, and the voltages will be better maintained within their rated limits, which will make it possible to increase the stability margins and to tend towards the thermal limits of the lines. However, the combination of PSSs and FACTS devices in the same network has raised a new problem in terms of coordination between these regulators. Indeed, it is essential to ensure that there is a good coordination between these devices in a way that their actions are not negative in view of the security of the network.

One of the well-known shunt FACTS devices, named static VAR compensator (SVC), is considered a competent device to provide adequate damping of the LFOs in modern power systems after the apparition of disturbances [4]. It also has the capability of regulating bus voltage at its terminals by injecting controllable reactive power into the power network through the bus where it is connected. In the last few years, many studies have proposed design techniques for SVC devices to enhance power system stability. Furthermore, other proprieties of the power system can be improved, such as the dynamic control of power flow, steady-state stability limits, and damping of electromechanical oscillations [5]. Most of these studies have been focused on the coordinated design of SVC and PSS controllers. Uncoordinated design between SVC and PSS causes the system to become unstable. There-fore, stability and damping modes are essential for optimal coordinated design between PSS and SVC-based controllers. A comprehensive study of the PSS and SVC controllers when applied in a coordinated manner and also separately has been investigated in [6]. The problem of designing the power system controller's parameters is formulated as a non-differentiable, large-scale nonlinear problem. This optimization problem is hard to solve by employing traditional optimization techniques such as sequential quadratic programming (SQP) techniques due to their high sensitivity to the initial point [7]. Furthermore, these methods require a long convergence process. To overcome the drawbacks mentioned, intelligent techniques are involved in real-life engineering problems, including power system stability [8–14].

Most of this research has been focused on the coordinated design of SVC and PSS controllers. For the coordinated design of power system controllers, a large number of such algorithms have recently been offered, including: Teaching–Learning Algorithm (TLA) [15], Bacterial Foraging Optimization (BFO) [16], Brainstorm optimization algorithm (BOA) [17], Coyote Optimization Algorithm (COA) [18], ant colony optimization (ACO) [19], bat algorithm (BAT) [20], bee colony algorithm (BCA) [7], Genetic Algorithm (GA) [21], particle swarm optimization (PSO) [22], flower pollination algorithm (FPA) [23], gravitational search algorithm (GSA) [24,25], sine-cosine algorithm (SCA) [26], grey wolf optimizer (GWO) [27], firefly algorithm (FA) [28], Differential Evolution (DE) [29], Biogeography-Based Optimization (BBO) [30], Cuckoo Search (CS) algorithm [31], Harmony Search (HS) [32], Seeker Optimization Algorithm (SOA) [33], Imperialist Competitive Algorithm (ICA) [34], Harris Hawk Optimization (HHO) [35], Sperm Swarm Optimization (SSO) [36], Tabu Search (TS) [37], Simulated Annealing [38], Multi-Verse Optimizer (MVO) [39], Moth-flame Optimization (MFO) [40], Tunicate

Swarm Algorithm (TSA) [41] and collective decision optimization (CDO) [42]. Although metaheuristics algorithms could provide relatively satisfactory results, no algorithm could provide superior performance than others in solving all optimizing problems. Therefore, several studies have been carried out to improve the performance and efficiency of the original metaheuristic algorithms in some ways and apply them for a specific purpose [43–48].

The SCA is a relatively new meta-heuristic optimization approach introduced by Mirjalili in 2016 [49]. Compared with other meta-heuristic, the SCA has a simple concept and structure and does not have complicated mathematical functions. In the SCA, the formulas for updating the population rely solely on sine and cosine functions. SCA is better than other competitive methods at finding optimal solutions and is suitable for tackling real-world optimization problems [50]. However, SCA tends to become trapped in local optima and, in some complex cases, is unable to successfully converge [51]. In addition, according to the No-Free-Lunch theorem [52], even though various optimization algorithms are introduced in the literature, there is no guarantee that an optimization algorithm could solve every kind of optimization problem. In other words, one algorithm or method cannot outperform others in all optimization problems. An optimization method may have satisfied results for some problems, but not for others. As a result, opportunities to introduce new methods will always exist. Therefore, in the current study an effective hybrid algorithm is developed based on the chaotic version of the SCA and pattern search (PS) method called hCSC-PS. The proposed hybrid algorithm utilizes the exploration ability of SCA and exploitation ability of PS, which can significantly improve the finding results. SCA and pattern search offer complementary benefits and the combination these two techniques can result in a faster and more reliable algorithm. To validate the efficacy of the new hybrid approach, a set of benchmark functions as well as controller design problems of a multi-machine power system are studied. Simulation results validate the superiority of the new method in design controllers under several loading situations.

The rest of this paper is organized as follows: Section 2 explains the proposed hybrid optimization algorithm. The problem is formulated as an optimization problem in Section 3. Section 4 discusses model verification. Section 5 contains a description of the simulation results. Finally, in Section 6, the study's findings are summarized.

2. Proposed Hybrid Algorithm

2.1. CSCA

SCA is a population-based metaheuristic technique based on the mathematical properties of sine and cosine functions [49]. This algorithm begins the search process with a collection of randomly generated solutions in the search space, as shown in the following equation.

$$x_i = lb_i + rand \times (ub_i - lb_i); \; i = 1, \, 2, \, \ldots, \, N \tag{1}$$

where x_i is the placement of ith solution in the search space. Furthermore, ub_i and lb_i represent the solution's lower and upper bounds, respectively. The parameters are defined in Appendix B. Following the generation of the random starting solutions, each solution dynamically modifies the positions using the equations below:

$$\begin{cases} x_i^{t+1} = x_i^t + A \times sin(r_1) \times \left| r_2 \times x_{Best} - x_i^t \right| & if \; r_3 < 0.5 \\ x_i^{t+1} = x_i^t + A \times cos(r_1) \times \left| r_2 \times x_{Best} - x_i^t \right| & otherwise \end{cases} \tag{2}$$

where, x_i^t is the position of ith solution at iteration t, x_{Best} represents the best solution in the population, r_1 is a random numbers in the range of $[0, 2\pi]$, r_2 is a random weight of the best solution among -2 and 2, r_3 is a random number among 0 and 1, and the symbol $| \, . \, |$ signifies absolute value. If the parameter r_3 is lesser than 0.5, the applicant solution selects

the sine function to update its position. The parameter A is a function that may be defined as follows to help balance the exploration and exploitation of a search space:

$$A = 2 - 2\left(\frac{t}{t_{max}}\right) \tag{3}$$

where, t_{max} is the maximum number of iterations. The aim of the current research is to implement the global search ability of the SCA. Therefore, to increase the exploration ability of the algorithm and to avoid premature convergence in early iterations, the chaotic sequence is applied in the updating position equation (Equation (2)). Chaotic systems are deterministic systems that present randomness, irregularity and the stochastic property, depending on the initial conditions. Chaotic variables can oscillate through certain ranges based on their own irregularity without repetition. A chaotic map is a map that presents some kind of chaotic behavior, capable of generating chaotic motion. In the current study, a well-known logistic map is applied based on the following equation:

$$\lambda\,(t+1) = a \times \lambda\,(t) \times (1 - \lambda\,(t)) \tag{4}$$

In this equation, $\lambda\,(t)$ is the chaotic map and t denotes the iteration number. $\lambda\,(0)$ is in the range of $(0, 1)$ and should not be equal to 0, 0.25, 0.5, 0.75 and 1. a is a constant equal to 4. In the CSCA, to increase the stochastic behavior of the algorithm and avoid premature convergence, the random parameters r_1 and r_2 in Equation (2) are changed with the chaotic map of Equation (4). Therefore, the updated position of the tunicate with respect to the position of the food source is evaluated using the Equation (5). The steps of the proposed CSCA are presented in Algorithm 1.

$$\begin{cases} x_i^{t+1} = x_i^t + A \times sin(\lambda_1) \times \left|\lambda_2 \times x_{Best} - x_i^t\right| & if\ r_3 < 0.5 \\ x_i^{t+1} = x_i^t + A \times cos(\lambda_1) \times \left|\lambda_2 \times x_{Best} - x_i^t\right| & otherwise \end{cases} \tag{5}$$

Algorithm 1. CSCA.

Initialization algorithm parameters: population size (N), maximum iteration number (t_{max}).
Initialize random population X
For $i = 1$ to N
       Calculate the fitness of each random solution
       Record the optimal individual as X_{best}
End
   While ($t \leq t_{max}$)
       Update A using Equation (3)
       Update λ using Equation (4)
       For $i = 1$ to N
           For $j = 1$ to dim
              Update r_3
              If $r_3 < 0.5$
                 Update X by the sine part of Equation (5)
              Else
                 Update X by the cosine part of Equation (5)
              End if
           End for
           Calculate the fitness of the updated X
         Update X_{best}
       End for
       $t = t + 1$
   End
Return the best solution

2.2. Pattern Search (PS)

PS is a derivative-free algorithm that can be simply implemented to fine-tune local search. The PS algorithm generates a set of points that may or may not be close to the optimum [53]. To begin, a mesh (a collection of points) is created around an existing point. If a new point in the mesh has a lower value of objective function, it becomes the current point in the following iteration. The PS starts the search with an initial point X_0 defined by the user. At the first iteration, the mesh size is considered equal to 1 and the pattern vectors (or direction vectors) are constructed as $[0\ 1] + X_0$, $[1\ 0] + X_0$, $[-1\ 0] + X_0$ and $[0\ -1] + X_0$, and new mesh points are added as presented in Figure 1. Then, the objective function is calculated for produced trial points until a value smaller than X_0 is found. If there is such a point ($f(X_1) < f(X_0)$), the poll is successful, and the algorithm sets this point as a source point. The method multiplies the current mesh size by 2 (called the expansion factor) after a successful poll and moves on to iteration 2 with the following new points: $2 \times [0\ 1] + X_1$, $2 \times [1\ 0] + X_1$, $2 \times [-1\ 0] + X_1$ and $2 \times [0\ -1] + X_1$. If a value lesser than for X_1 is created, X_2 is defined, the mesh size is improved by two, and iterations continue. The current point is not modified if the poll is unsuccessful at any stage (i.e., no point has an objective function lesser than the greatest latest rate) and the mesh size is reduced by multiplying by a reduction factor. This process is repeated until the minimum is found or a terminating conditions is met. The steps of the PS method are presented in Algorithm 2.
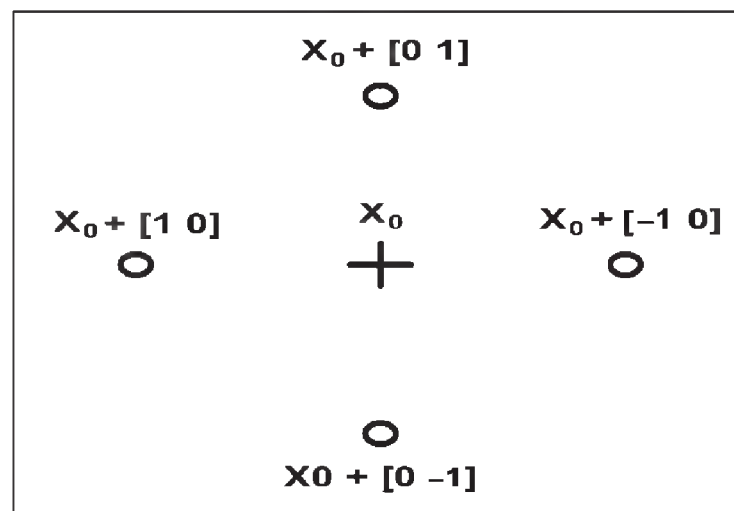
Figure 1. Pattern search mesh points with pattern.

Algorithm 2. Pattern search method.

Initialization:
  Initialize the starting point X_0 and step size factor SF
  Set $t = 0$
Iteration:
1. Search step: evaluate f at a finite number of points with the goal of decreasing the objective function value at X_k. If X_{k+1} is found satisfying $f(X_{k+1}) < f(X_k)$, go to step 4.
Otherwise, go to step 2.
2. Poll step: If $f(X_k) \leq f(X)$ for every X in the mesh neighborhood, go to step 3.
    Otherwise, choose a point X_{k+1} such that $f(X_{k+1}) < f(X_k)$, go to step 4.
3. Mesh reduction: let $SF_{k+1} = 1/2 \times SF_k$. Set $k \leftarrow k + 1$ and return to step 1 for a new iteration.
4. Mesh expansion: let $SF_{k+1} = 2 \times SF_k$. Set $k \leftarrow k + 1$ and return to step 1 for a new iteration

---

2.3. Proposed Method (hCSC-PS)

The original SCA has some advantages compared with other optimization algorithms. It has a simple structure and fewer parameters. In addition, the performance of the algorithm depends on the sine and cosine functions for iteration to find the optimal solution. Although the original SCA has high global search capabilities, its parameters are incompatible with the search process in the latter stages of the algorithm. This will reduce the rate of convergence and population diversity. In this study, a hybrid algorithm combining the CSCA with the PS algorithm, called hCSC-PS, is proposed for the coordinated design of PSSs and SVC-based controllers. The hybrid algorithm may take advantage of both the CSCA's strong global searching capacity and the PS's strong local searching ability. The chaotic sine cosine method has excellent global optimal performance and is easy to escape from local minima. Theoretically, increasing the numbers of CSCA iteration can improve the search accuracy. When the number of iterations is great enough, however, CSCA is unable to enhance precision. As a result, CSCA's local search capability is still insufficient. Pattern search is a local optimization approach, and the initial point has a significant impact on the algorithm's output. However, if a good starting point is chosen, pattern search will be a simple and effective strategy. In this study, we integrate the CSCA's benefits as global optimization and PS's advantages as the local optimization to effectively find the optimal solution. The proposed hybrid algorithm begins with the CSCA since the PS is sensitive to the initial solution. The searching process continues with the CSCA for a specific number of iterations. The PS is then turned on to conduct a local search using the current best solution obtained by CSCA as its starting point. The suggested hCSC-PS algorithm's flowchart is given in Figure 2.
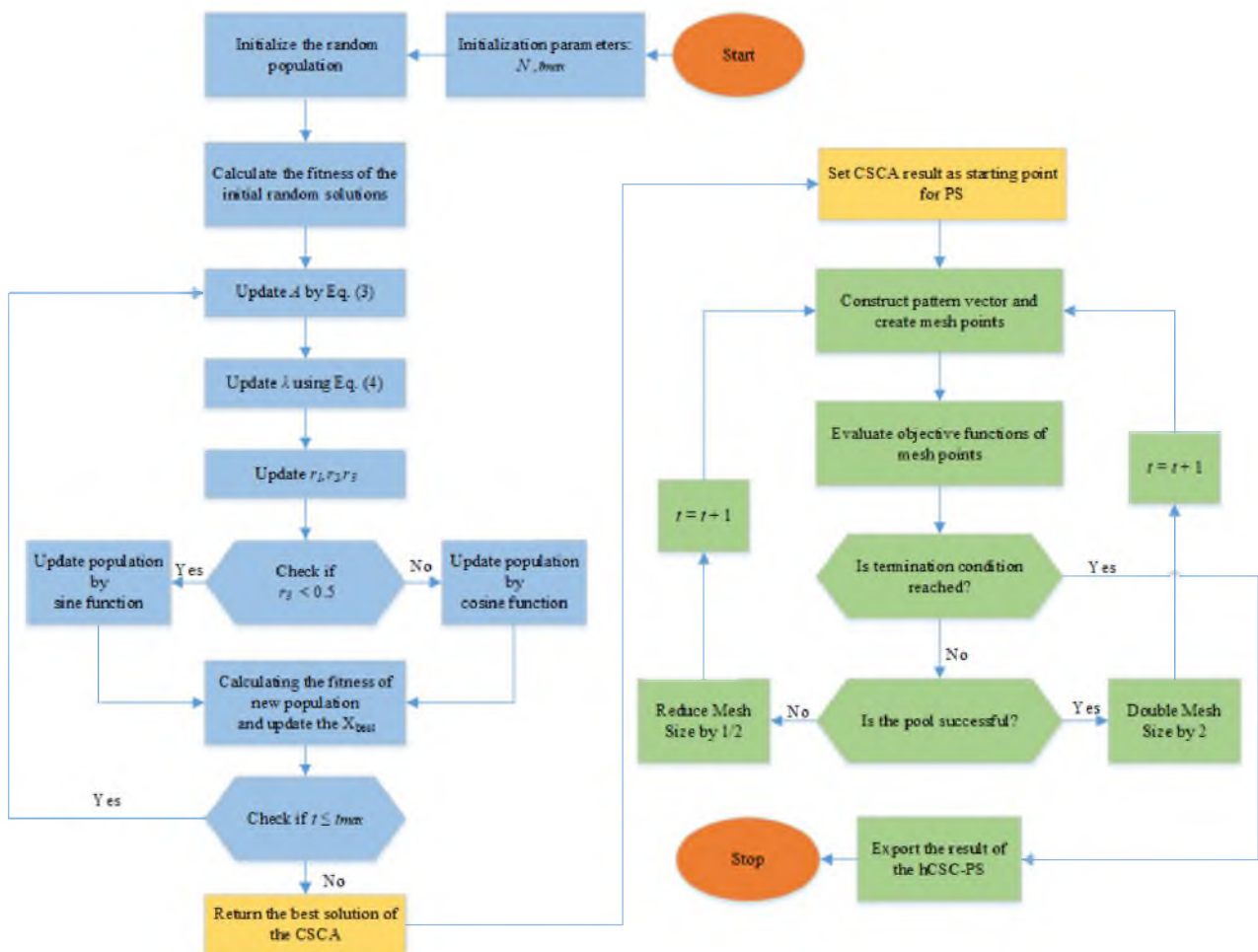

Figure 2. The flowchart of the proposed hCSC-PS algorithm.

3. Optimization Problem Formulation

The general form of a constraint optimization problem can be expressed mathematically as follows:

$$
\begin{aligned}
&minimize\ \ f(X)\\
&subject\ to\\
&g_i(X) \leq 0.\quad i = 1,2,\ldots,p\\
&h_j(X) \leq 0.\quad j = 1,2,\ldots,m\\
&X^L \leq X \leq X^U
\end{aligned}
\tag{6}
$$

where X is n dimensional vector of design variables, $f(X)$ is the fitness function which returns a scalar value to be minimized, $g(X)$ and $h(X)$ are inequality and equality constraints, respectively. Boundary constraints, X^L and X^U, are the boundary constraints. Many optimization methods have been developed over the last few decades. Metaheuristics are a new generation of optimization methods that are proposed to solve complex problems.

3.1. Power System Model

The standard modeling for power systems is based on a set of nonlinear differential algebraic calculations, which are as follows:

$$
\dot{X} = f(X.U)
\tag{7}
$$

where $X = [\delta,\ \omega,\ E_q,\ E_{fd}]$ is the state variables vector and $U = [u_{PSS},\ u_{svc}]$ is the input control parameters vector. The linear equation with PSSs and SVC controllers is obtained by Equation (8).

$$
\dot{X} = AX + BU
\tag{8}
$$

At a certain operating point, both A and B are evaluated. The goal of the optimum design is to put the state matrix modes on the left side.

3.1.1. PSS Structure

PSS compensates for the phase lag between exciter input and machine electrical torque. An additional stabilizing signal is presented through the excitation system to achieve this goal. PSS generates the necessary torque on the machine's rotor. The additional stabilizing signal and the speed are proportional. As shown in Figure 3, this stabilizer style contains of a washout filter and a dynamic compensator. The washout filter, which is primarily a high pass filter, will remove the mean component of PSS's output. In general, the constant value of time can be anywhere between 0.5 and 20 s.
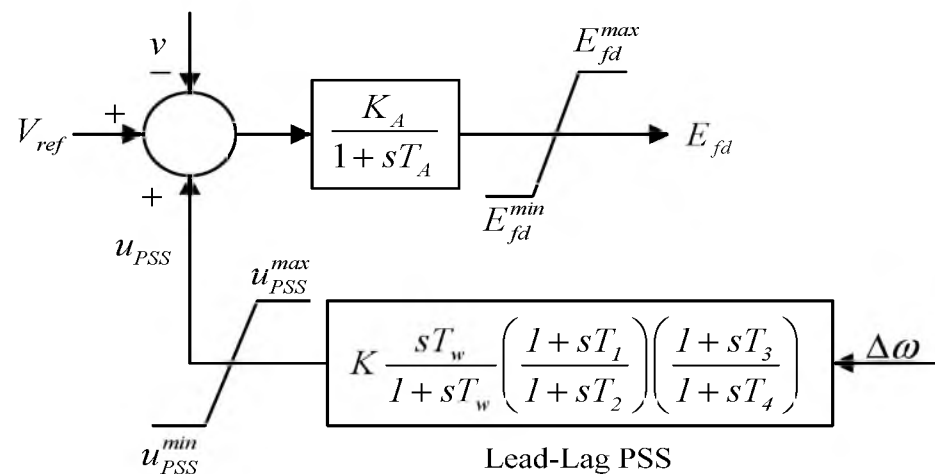
Figure 3. Lead/Lag PSS.

3.1.2. SVC Based Damping Controller Model

Figure 4 shows the SVC structure in this study, which is a fixed capacitor thyristor-controlled reactor. The firing angle varies between 90 and 180 degrees depending on the capacitor voltage.
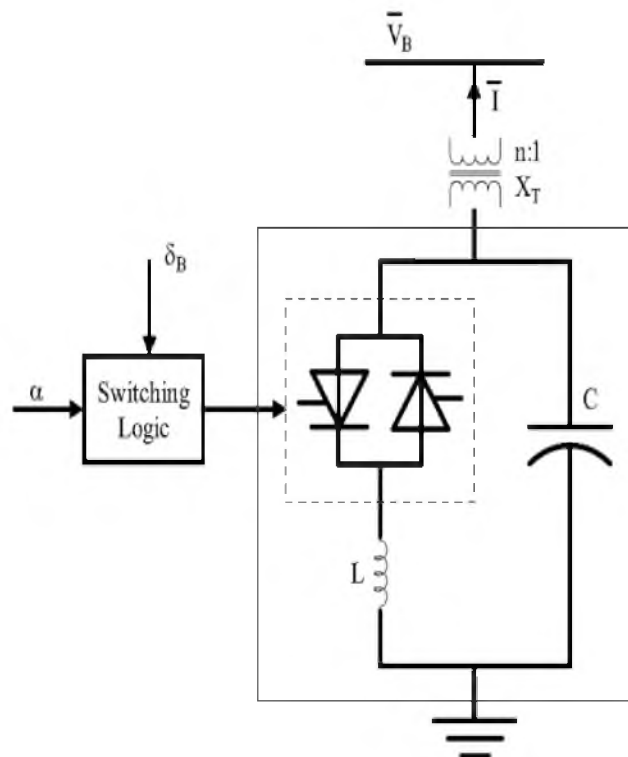
Figure 4. Modeling the SVC.

Figure 5 shows an SVC-based damping controller that acts as a lead-lag compensator and consists of two stages of the lead-lag compensator: a signal-washout block, and a gains block. SVC has the following dynamic equation:

$$\dot{B}_{SVC} = \left(K_s \left(B_{SVC}^{ref} - u_{SVC} \right) - B_{SVC} \right) / T_s \tag{9}$$
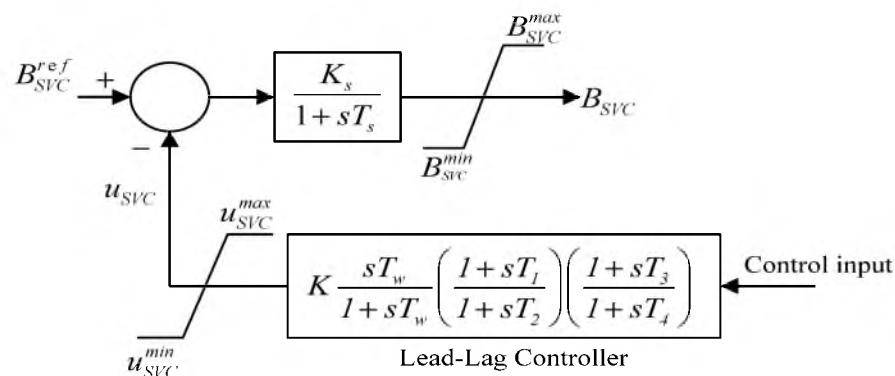
Figure 5. SVC with lead–lag controller.

3.2. Problem Formulation

The optimum parameters are obtained using the suggested technique under a variety of operating conditions and disturbances. For the optimal setting of PSSs and SVC con-

trollers, a nonlinear time domain objective function called ITAE is used in this study. The equation can be used to define ITAE based on system performance characteristics (10).

$$J = \sum_{j=1}^{N} \sum_{i=1}^{M} \int_{0}^{t_{sim}} t(|\Delta\omega_i|)dt \tag{10}$$

where $\Delta\omega$ is the speed deviation of rotor, t_{sim} is the time of simulation, N and M are the number of machine and the operating points respectively. The objective function and constrained optimization problem can be described by the following equation for various loading conditions:

$$
\begin{aligned}
& minimize \quad J \\
& \quad subject\ to \\
& K_i^{min} \le K_i \le K_i^{max} \\
& T_{ji}^{min} \le T_{ji} \le T_{ji}^{max} \quad j = 1, \dots, 4
\end{aligned}
\tag{11}
$$

hCSC-PS determines the gain (K) and time constants (T) of controllers. The washout time constant for both PSS and SVC controllers is $T_{Wi} = 10$ s in most previous works. The decision variables' typical ranges are [1, 100] for K_i and [0.01, 1.5] for T_{1i} to T_{4i}.

4. Performance Verification of hCSC-PS

In this section the effectiveness verification of the proposed hybrid method will be investigated. To this aim, the performance of hCSC-PS is compared with the standard version of the algorithm as well as some well-known metaheuristic algorithms on a collection of benchmark test functions from the literature. These are all minimization problems that can be used to assess the robustness and search efficiency of new optimization algorithms. Tables 1–3 show the mathematical formulation and features of these test functions.

Table 1. Description of unimodal benchmark functions.
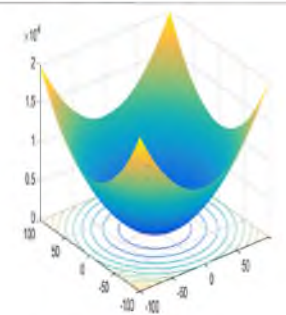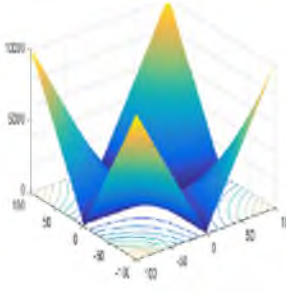
Function	Range	f_{min}	n (Dim)	3D View
$F_1(X) = \sum_{i=1}^{n} x_i^2$	$[-100, 100]^n$	0	30	
$F_2(X) = \sum_{i=1}^{n}|x_i| + \prod_{i=1}^{n}|x_i|$	$[-10, 10]^n$	0	30	

Table 1. *Cont.*
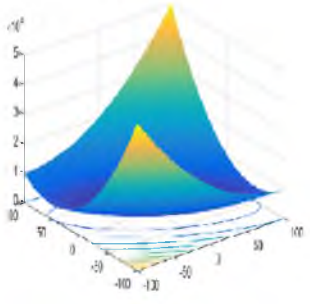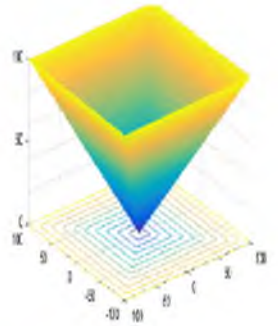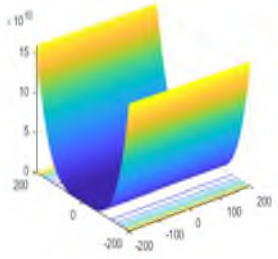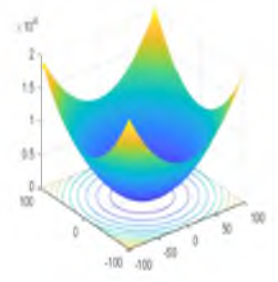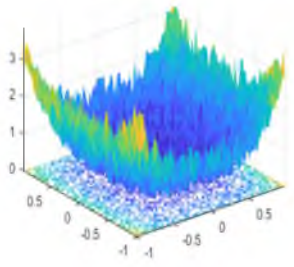
Function	Range	f_{min}	n (Dim)	3D View
$F_3(X) = \sum_{i=1}^{n} \left(\sum_{j=1}^{i} x_j \right)^2$	$[-100, 100]^n$	0	30	
$F_4(X) = \max_i \left\{ |x_i|. \, 1 \leq i \leq n \right\}$	$[-100, 100]^n$	0	30	
$F_5(X) = \sum_{i=1}^{n-1} \left[100\left(x_{i+1} - x_i^2\right)^2 + (x_i - 1)^2 \right]$	$[-30, 30]^n$	0	30	
$F_6(X) = \sum_{i=1}^{n} \left([x_i + 0.5] \right)^2$	$[-100, 100]^n$	0	30	
$F_7(X) = \sum_{i=1}^{n} i x_i^4 + random[0.1)$	$[-1.28, 1.28]^n$	0	30	

Table 2. Description of multimodal benchmark functions.
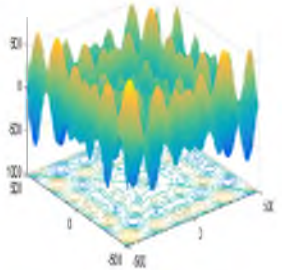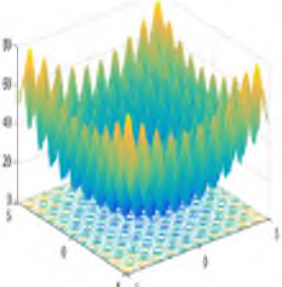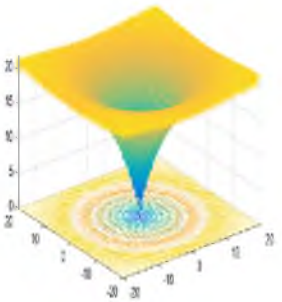
Function	Range	f_{min}	n (Dim)	3D View
$F_8(X) = \sum_{i=1}^{n} -x_i \sin\left(\sqrt{\lvert x_i \rvert}\right)$	$[-500,\ 500]^n$	$428.9829 \times n$	30	
$F_9(X) = \sum_{i=1}^{n} \left[x_i^2 - 10 \cos(2\pi x_i) + 10 \right]$	$[-5.12,\ 5.12]^n$	0	30	
$F_{10}(X) = -20 \exp\left(-0.2\sqrt{\frac{1}{n}\sum_{i=1}^{n} x_i^2}\right) - exp\left(\frac{1}{n}\sum_{i=1}^{n}\cos(2\pi x_i)\right) + 20 + e$	$[-32,\ 32]^n$	0	30	

Table 2. *Cont.*
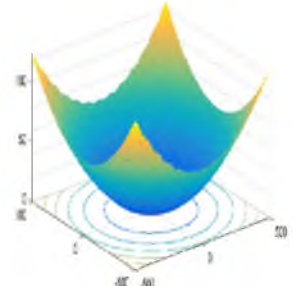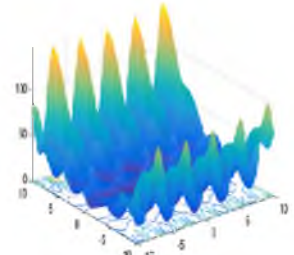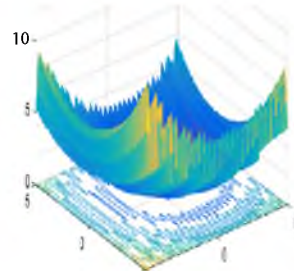
Function	Range	f_{min}	n (Dim)	3D View
$F_{11}(X) = \frac{1}{4000} \sum_{i=1}^{n} x_i^2 - \prod_{i=1}^{n} \cos\left(\frac{x_i}{\sqrt{i}}\right) + 1$	$[-600, 600]^n$	0	30	
$F_{12}(X) = \frac{\pi}{n} \left\{ 10 \sin(\pi y_1) + \sum_{i=1}^{n-1} (y_i - 1)^2 \left[1 + 10 \sin^2(\pi y_{i+1})\right] + (y_n - 1)^2 \right\} + \sum_{i=1}^{n} u(x_i. 10. 100. 4)$ $y_i = 1 + \frac{x_{i+1}}{4} u(x_i, a. k. m) = \begin{cases} k(x_i - a)^m & x_i > a \\ 0 & a < x_i < a \\ k(-x_i - a)^m & x_i < -a \end{cases}$	$[-50, 50]^n$	0	30	
$F_{13}(X) = 0.1\left\{ \sin^2(3\pi x_1) + \sum_{i=1}^{n} (x_i - 1)^2 \left[1 + \sin^2(3\pi x_i + 1)\right] + (x_n - 1)^2 \left[1 + \sin^2(2\pi x_n)\right] \right\} + \sum_{i=1}^{n} u(x_i. 5. 100. 4)$	$[-50, 50]^n$	0	30	

Table 3. Description of fixed-dimension multimodal benchmark functions.
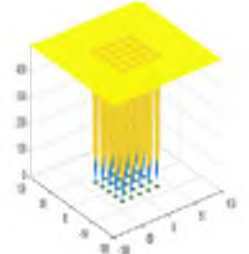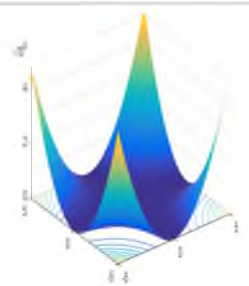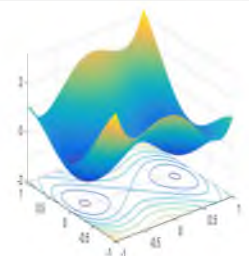
Function	Range	f_{min}	n (Dim)	3D View
$F_{14}(X) = \left(\frac{1}{500} + \sum_{j=1}^{25} \frac{1}{j + (x_i - a_{ij})^6} \right)^{-1}$	$[-65.53,\ 65.53]^2$	1	2	
$F_{15}(X) = \sum_{i=1}^{11} \left[a_i - \frac{x_1(b_i^2 + b_i x_2)}{b_i^2 + b_i x_3 + x_4} \right]^2$	$[-5,\ 5]^4$	0.00030	4	
$F_{16}(X) = 4x_1^2 - 2.1x_1^4 + \frac{1}{3}x_1^6 + x_1 x_2 - 4x_2^2 + 4x_2^4$	$[-5,\ 5]^2$	-1.0316	2	

Table 3. *Cont.*
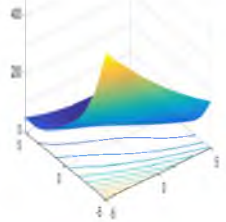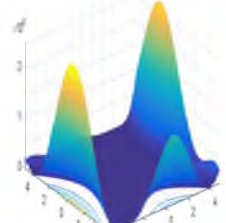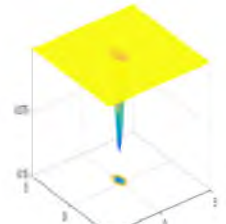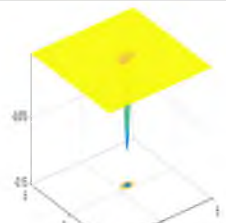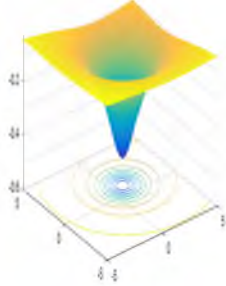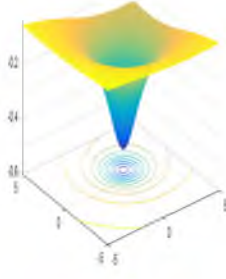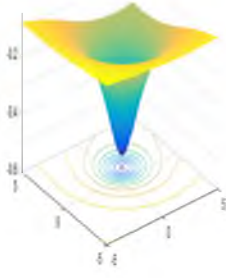
Function	Range	f_{min}	n (Dim)	3D View
$F_{17}(X) = \left(x_2 - \frac{5.1}{4\pi^2}x_1^2 + \frac{5}{\pi}x_1 - 6\right)^2 + 10\left(1 - \frac{1}{8\pi}\right)\cos x_1 + 10$	$[-5, 5]^2$	0.398	2	
$F_{18}(X) = \left[1 + (x_1 + x_2 + 1)^2\left(19 - 14x_1 + 3x_1^2 - 14x_2 + 6x_1x_2 + 3x_2^2\right)\right] \times$ $\left[30 + (2x_1 - 3x_2)^2 \times \left(18 - 32x_1 + 12x_1^2 + 48x_2 - 36x_1x_2 + 27x_2^2\right)\right]$	$[-2, 2]^2$	3	2	
$F_{19}(X) = -\sum_{i=1}^{4} c_i \, exp\left(-\sum_{j=1}^{3} a_{ij}\left(x_j - p_{ij}\right)\right)^2$	$[1, 3]^3$	-3.86	3	
$F_{20}(X) = -\sum_{i=1}^{4} c_i \, exp\left(-\sum_{j=1}^{6} a_{ij}\left(x_j - p_{ij}\right)\right)^2$	$[0, 1]^6$	-3.32	6	

Table 3. *Cont.*

Function	Range	f_{min}	n (Dim)	3D View
$F_{21}(X) = -\sum_{i=1}^{5}\left[(X-a_i)(X-a_i)^T + c_i\right]^{-1}$	$[0, 10]^n$	-10.1532	4	
$F_{22}(X) = -\sum_{i=1}^{7}\left[(X-a_i)(X-a_i)^T + c_i\right]^{-1}$	$[0, 10]^n$	-10.4028	4	
$F_{23}(X) = -\sum_{i=1}^{10}\left[(X-a_i)(X-a_i)^T + c_i\right]^{-1}$	$[0, 10]^n$	-10.5363	4	

The results and performance of the proposed hCSC-PS is compared with original SCA and other well-established optimization algorithms include GSA [54], TSA [55] and, GWO [56]. For both hCSC-PS and SCA the size of solution (N) is considered equal to 50. As the proposed algorithm required extra function evaluation, the same value of maximum number of iterations may cause an unfair comparison. Therefore, to have a fair comparison between the algorithms, the same number of function evaluations equal to 50,000 is considered in all experiments. The parameters of the hCSC-PS and other methods are presented in Table 4. Because metaheuristics approaches are stochastic, the findings of a single run may be erroneous, and the algorithms may find better or worse solutions than those previously found. As a result, statistical analysis should be used to make a fair comparison and evaluate the algorithms' effectiveness. In order to address this issue, 30 separate runs were carried out for the specified algorithms and the statistical outcomes are described in Tables 5–7.

Table 4. Bound setting of the proposed methods.

Year	Algorithm	Parameter	Specifications
2021	hCSC-PS	Search agents	50
		Number of elites	2
		Number of function evaluations	50,000
2016	SCA	Search agents	50
		Number of elites	2
		Number of function evaluations	50,000
2009	GSA	Search agents	50
		Gravitational constant	100
		Alpha coefficient	20
		Number of function evaluations	50,000
2014	GWO	Search agents	50
		Control parameter ($\vec{a}$)	[2,0]
		Number of function evaluations	50,000
2020	TSA	Search agents	50
		Parameter $Pmin$	1
		Parameter $Pmax$	4
		Number of function evaluations	50,000

Table 5. Comparison of other techniques in resolving multimodal test functions in Table 1.

Function	Statistics	hCSC-PS	SCA	GSA	TSA	GWO
F_1	Best	0.000	1.551×10^{-6}	1.101×10^{-17}	5.145×10^{-60}	2.391×10^{-61}
	Worst	0.000	2.030×10^{-3}	3.186×10^{-17}	1.058×10^{-55}	3.564×10^{-58}
	Mean	0.000	2.340×10^{-5}	2.117×10^{-17}	8.215×10^{-55}	4.116×10^{-59}
	Median	0.000	1.874×10^{-4}	2.007×10^{-17}	7.401×10^{-55}	1.153×10^{-59}
	Std.	0.000	7.929×10^{-5}	5.815×10^{-17}	2.390×10^{-55}	1.123×10^{-58}
F_2	Best	0.000	1.500×10^{-6}	1.528×10^{-8}	1.119×10^{-35}	8.362×10^{-36}
	Worst	0.000	9.830×10^{-6}	3.331×10^{-8}	3.281×10^{-32}	5.340×10^{-34}
	Mean	0.000	1.687×10^{-6}	2.393×10^{-8}	2.151×10^{-33}	8.361×10^{-35}
	Median	0.000	5.402×10^{-7}	2.347×10^{-8}	3.104×10^{-34}	5.929×10^{-35}
	Std.	0.000	2.304×10^{-6}	4.002×10^{-8}	6.023×10^{-33}	9.850×10^{-35}
F_3	Best	0.000	7.172×10	1.029×10^2	2.568×10^{-32}	1.253×10^{-19}
	Worst	0.000	2.660×10^3	4.686×10^2	2.449×10^{-17}	3.557×10^{-13}
	Mean	0.000	7.991×10^2	2.454×10^2	8.174×10^{-19}	1.509×10^{-14}
	Median	0.000	6.294×10^2	2.211×10^2	1.869×10^{-24}	2.074×10^{-17}
	Std.	0.000	7.562×10^2	1.001×10^2	4.471×10^{-18}	6.554×10^{-14}

Table 5. *Cont.*

Function	Statistics	hCSC-PS	SCA	GSA	TSA	GWO
F_4	Best	**0.000**	1.161	2.230×10^{-9}	3.235×10^{-8}	9.821×10^{-16}
	Worst	**0.000**	3.467×10	5.085×10^{-9}	6.342×10^{-5}	2.441×10^{-13}
	Mean	**0.000**	9.208	3.303×10^{-9}	1.011×10^{-5}	1.948×10^{-14}
	Median	**0.000**	6.080	3.200×10^{-9}	2.027×10^{-6}	6.381×10^{-15}
	Std.	**0.000**	8.672	7.444×10^{-9}	1.692×10^{-5}	4.491×10^{-14}
F_5	Best	$\mathbf{5.061 \times 10^{-1}}$	2.712×10	2.574×10	2.562×10	2.521×10
	Worst	$\mathbf{8.123 \times 10^{-1}}$	4.951×10	2.209×10^2	2.954×10	2.872×10
	Mean	$\mathbf{7.183 \times 10^{-1}}$	2.911×10	4.228×10	2.844×10	2.690×10
	Median	$\mathbf{7.270 \times 10^{-1}}$	2.900×10	2.617×10	2.891×10	2.713×10
	Std.	$\mathbf{1.063 \times 10^{-1}}$	4.152	4.544×10	7.619×10^{-1}	8.408×10^{-1}
F_6	Best	**0.000**	3.457	9.712×10^{-18}	2.054	2.456×10^{-1}
	Worst	**0.000**	4.843	8.642×10^{-17}	4.772	1.291
	Mean	**0.000**	4.436	3.097×10^{-17}	3.670	6.476×10^{-1}
	Median	**0.000**	4.457	2.933×10^{-17}	3.561	7.252×10^{-1}
	Std.	**0.000**	2.850×10^{-1}	6.169×10^{-17}	0.693	3.053×10^{-1}
F_7	Best	$\mathbf{3.305 \times 10^{-10}}$	4.150×10^{-2}	8.100×10^{-3}	6.710×10^{-4}	1.523×10^{-4}
	Worst	$\mathbf{1.221 \times 0^{-14}}$	3.100×10^{-3}	9.620×10^{-2}	3.100×10^{-2}	4.200×10^{-2}
	Mean	$\mathbf{7.280 \times 0^{-16}}$	4.116×10^{-1}	3.370×10^{-2}	4.800×10^{-2}	7.995×10^{-4}
	Median	$\mathbf{3.300 \times 0^{-10}}$	8.780×10^{-2}	1.220×10^{-2}	5.800×10^{-2}	7.069×10^{-4}
	Std.	$\mathbf{2.488 \times 10^{-5}}$	5.010×10^{-2}	8.800×10^{-3}	7.7266×10^{-4}	4.678×10^{-4}

Table 6. Comparison of other techniques in resolving multimodal test functions in Table 2.

Function	Statistics	hCSC-PS	SCA	GSA	TSA	GWO
F_8	Best	$\mathbf{-1.100 \times 10^4}$	-5.399×10^3	-3.627×10^3	-7.999×10^3	-8.917×10^3
	Worst	$\mathbf{-1.001 \times 10^4}$	-3.432×10^3	-2.103×10^3	-5.376×10^3	-4.878×10^3
	Mean	$\mathbf{-1.100 \times 10^4}$	-4.576×10^3	-2.882×10^3	-6.412×10^3	-6.357×10^3
	Median	$\mathbf{-1.102 \times 10^4}$	-3.672×10^3	-2.846×10^3	-6.513×10^3	-6.426×10^3
	Std.	$\mathbf{1.734 \times 10^2}$	3.768×10^2	3.754×10^2	5.692×10^{23}	8.524×10^{23}
F_9	Best	**0.000**	1.066×10^{-6}	8.854	7.877×10	0.000
	Worst	**0.000**	4.143×10	2.788×10	2.949×10^2	1.105×10
	Mean	**0.000**	5.969	1.672×10	1.014×10^2	8.553×10^{-1}
	Median	**0.000**	8.339×10^{-4}	1.531×10	1.096×10^2	0.000
	Std.	**0.000**	1.124×10	3.204	3.387×10	2.4938
F_{10}	Best	$\mathbf{8.881 \times 10^{-16}}$	1.556×10^{-5}	2.428×10^{-9}	1.569×10^{-14}	1.560×10^{-14}
	Worst	$\mathbf{8.881 \times 10^{-16}}$	2.121×10	4.582×10^{-9}	4.012	2.020×10^{-14}
	Mean	$\mathbf{8.881 \times 10^{-16}}$	1.336×10	4.691×10^{-9}	2.409	1.547×10^{-15}
	Median	$\mathbf{8.881 \times 10^{-16}}$	2.112×10	3.486×10^{-9}	2.765	1.459×10^{-14}
	Std.	**0.000**	7.977	5.133×10^{-10}	1.097	2.376×10^{-15}
F_{11}	Best	**0.000**	4.348×10^{-7}	1.654	0.00	0.000
	Worst	**0.000**	7.654×10^{-1}	1.028×10	1.090×10^{-2}	8.400×10^{-2}
	Mean	**0.000**	2.148×10^{-1}	4.452	6.700×10^{-2}	9.400×10^{-3}
	Median	**0.000**	1.320×10^{-2}	3.565	7.200×10^{-2}	0.000
	Std.	**0.000**	2.218×10^{-1}	2.023	5.700×10^{-2}	4.100×10^{-3}
F_{12}	Best	$\mathbf{4.611 \times 10^{-32}}$	2.456×10^{-1}	8.214×10^{-20}	2.876×10^{-1}	2.540×10^{-2}
	Worst	$\mathbf{4.611 \times 10^{-32}}$	5.632	1.343×10^{-1}	1.398×10	4.200×10^{-2}
	Mean	$\mathbf{4.611 \times 10^{-32}}$	9.654×10^{-1}	4.580×10^{-2}	6.094	6.640×10^{-2}
	Median	$\mathbf{4.611 \times 10^{-32}}$	4.209×10^{-1}	1.303×10^{-19}	6.765	8.290×10^{-2}
	Std.	$\mathbf{1.044 \times 10^{-47}}$	1.144	4.230×10^{-2}	3.409	5.010×10^{-2}
F_{13}	Best	$\mathbf{1.245 \times 10^{-32}}$	1.945	1.354×10^{-18}	1.9876	1.001×10^{-1}
	Worst	$\mathbf{1.000 \times 10^{-2}}$	2.298×10	1.000×10^{-2}	3.2305	1.041
	Mean	$\mathbf{5.000 \times 10^{-3}}$	3.541	6.334×10^{-4}	1.9976	5.283×10^{-1}
	Median	$\mathbf{1.000 \times 10^{-2}}$	2.366	2.109×10^{-18}	1.8574	5.235×10^{-1}
	Std.	$\mathbf{4.000 \times 10^{-3}}$	3.980	1.800×10^{-2}	6.436×10^{-1}	3.351×10^{-1}

Table 7. Comparison of other techniques in resolving multimodal test functions in Table 3.

Function	Statistics	hCSC-PS	SCA	GSA	TSA	GWO
F_{14}	Best	$\mathbf{9.980 \times 10^{-1}}$	9.980×10^{-1}	9.980×10^{-1}	9.980×10^{-1}	9.980×10^{-1}
	Worst	$\mathbf{9.980 \times 10^{-1}}$	2.982	8.085	1.267×10	1.267×10
	Mean	$\mathbf{9.980 \times 10^{-1}}$	1.196	3.621	7.665	4.131
	Median	$\mathbf{9.980 \times 10^{-1}}$	9.980×10^{-1}	3.045	1.076×10	2.982
	Std.	$\mathbf{1.472 \times 10^{-11}}$	6.054×10^{-1}	2.194	4.884	4.144
F_{15}	Best	$\mathbf{3.138 \times 10^{-4}}$	3.406×10^{-4}	1.200×10^{-2}	3.751×10^{-4}	3.174×10^{-4}
	Worst	$\mathbf{3.968 \times 10^{-4}}$	1.400×10^{-2}	1.180×10^{-1}	5.660×10^{-2}	2.040×10^{-2}
	Mean	$\mathbf{3.364 \times 10^{-4}}$	8.597×10^{-4}	2.500×10^{-2}	4.300×10^{-2}	4.400×10^{-2}
	Median	$\mathbf{3.232 \times 10^{-4}}$	7.309×10^{-4}	2.100×10^{-2}	4.539×10^{-4}	3.075×10^{-4}
	Std.	$\mathbf{2.458 \times 10^{-5}}$	3.808×10^{-4}	1.900×10^{-2}	1.160×10^{-1}	8.100×10^{-2}
F_{16}	Best	$\mathbf{-1.031}$	-1.031	-1.031	-1.031	-1.031
	Worst	$\mathbf{-1.031}$	-1.031	-1.031	-1.000	-1.031
	Mean	$\mathbf{-1.031}$	-1.031	-1.031	-1.030	-1.031
	Median	$\mathbf{-1.031}$	-1.031	-1.031	-1.031	-1.031
	Std.	1.859×10^{-6}	1.039×10^{-5}	5.608×10^{-5}	5.800×10^{-2}	$\mathbf{4.738 \times 10^{-9}}$
F_{17}	Best	$\mathbf{3.979 \times 10^{-1}}$	3.979×10^{-1}	$\mathbf{3.979 \times 10^{-1}}$	3.979×10^{-1}	3.979×10^{-1}
	Worst	$\mathbf{3.979 \times 10^{-1}}$	3.992×10^{-1}	$\mathbf{3.979 \times 10^{-1}}$	3.980×10^{-1}	3.979×10^{-1}
	Mean	$\mathbf{3.979 \times 10^{-1}}$	3.982×10^{-1}	$\mathbf{3.979 \times 10^{-1}}$	3.979×10^{-1}	3.979×10^{-1}
	Median	$\mathbf{3.979 \times 10^{-1}}$	3.982×10^{-1}	$\mathbf{3.979 \times 10^{-1}}$	3.979×10^{-1}	3.979×10^{-1}
	Std.	$\mathbf{0.000}$	3.488×10^{-4}	$\mathbf{0.000}$	1.371×10^{-5}	1.105×10^{-6}
F_{18}	Best	$\mathbf{3.000}$	$\mathbf{3.000}$	$\mathbf{3.000}$	3.000	3.000
	Worst	$\mathbf{3.000}$	$\mathbf{3.000}$	$\mathbf{3.000}$	8.400×10	3.000
	Mean	$\mathbf{3.000}$	$\mathbf{3.000}$	$\mathbf{3.000}$	5.700	3.000
	Median	$\mathbf{3.000}$	$\mathbf{3.000}$	$\mathbf{3.000}$	3.000	3.000
	Std.	1.098×10^{-14}	5.349×10^{-6}	1.592×10^{-15}	14.7885	9.505×10^{-6}
F_{19}	Best	$\mathbf{-3.862}$	-3.862	-3.862	-3.862	-3.862
	Worst	$\mathbf{-3.862}$	-3.854	-3.862	-3.954	-3.954
	Mean	$\mathbf{-3.862}$	-3.875	-3.862	-3.062	-3.962
	Median	$\mathbf{-3.862}$	-3.806	-3.862	-3.962	-3.962
	Std.	$\mathbf{4.186 \times 10^{-16}}$	2.800×10^{-2}	2.479×10^{-5}	1.500×10^{-2}	2.100×10^{-2}
F_{20}	Best	$\mathbf{-3.322}$	-3.191	-3.322	-3.321	-3.322
	Worst	$\mathbf{-3.322}$	-2.048	-1.855	-3.088	-3.029
	Mean	$\mathbf{-3.322}$	-3.015	-2.953	-3.253	-3.249
	Median	$\mathbf{-3.322}$	-3.013	-2.987	-3.202	-3.262
	Std.	$\mathbf{1.355 \times 10^{-15}}$	1.974×10^{-1}	2.446×10^{-1}	6.710×10^{-2}	8.210×10^{-2}
F_{21}	Best	$\mathbf{-1.015 \times 10}$	-8.137	-1.015×10	-1.013×10	-1.015×10
	Worst	$\mathbf{-1015 \times 10}$	-8.800×10^{-1}	-2.682	-2.666	-5.099
	Mean	$\mathbf{-1.015 \times 10}$	-4.318	-6.396	-7.287	-9.479
	Median	$\mathbf{-1.015 \times 10}$	-4.905	-3.954	-7.419	-1.015×10
	Std.	$\mathbf{2.499 \times 10^{-17}}$	2.078	3.590	2.859	1.746
F_{22}	Best	$\mathbf{-1.040 \times 10}$	-9.054	-1.040×10	-1.039×10	-1.040×10
	Worst	$\mathbf{-1.040 \times 10}$	-9.064×10^{-1}	-1.040×10	-2.748	-5.085
	Mean	$\mathbf{-1.040 \times 10}$	-5.415	-1.040×10	-7.838	-1.022×10
	Median	$\mathbf{-1.040 \times 10}$	-5.037	-1.040×10	-1.025×10	-1.040×10
	Std.	$\mathbf{5.420 \times 10^{-15}}$	1.738	4.661×10^{-6}	3.184	9.723×10^{-1}
F_{23}	Best	$\mathbf{-1.053 \times 10}$	-9.3851	-1.053×1.0	-1.051×10	-1.053×10
	Worst	$\mathbf{-1.053 \times 10}$	-3.2531	-1053×10	-1.675	-1.053×10
	Mean	$\mathbf{-1.053 \times 10}$	-5.2925	-1.053×10	-7.673	-1.053×10
	Median	$\mathbf{-1.053 \times 10}$	-5.0398	-1.053×10	-1.041×10	-1.053×10
	Std.	$\mathbf{2.485 \times 10^{-18}}$	1.0982	1.836×10^{-15}	3.7585	2.585×10^{-4}

The results of Tables 5–7 show that, for all functions, hCSC-PS could provide better solutions in terms of the best and the mean value of the objective functions compared with the standard SCA and also other optimization algorithms. The results show that hCSC-PS is a more stable approach than the other methods in terms of standard deviation, which indicates the algorithm's stability. Based on the findings, it can be inferred that hCSC-PS outperforms the standard algorithm as well as alternative optimization methods.

5. Practical Applications

Figure 6 shows a single-line diagram of the 3-machine 9-bus (WSCC), which is used to demonstrate the proposed technique's efficacy and robustness [5,57]. Different strategies for determining the best location for SVCs devices have been described in the literature [5]. The WSCC system was subjected to two strategies based on the effect of load percentage and line outage on load bus voltages, with bus number 5 being selected as the best location for the SVC device. The proposed controllers' performance is evaluated using four different loading conditions. Table 8 shows four operating conditions (cases), which they are considered as representative cases in the literature [5,15,18,44], for evaluating the performance of the proposed controllers. These operating conditions are considered for the WSCC test system in the design process. The dynamics model of the system is given in Appendix A.
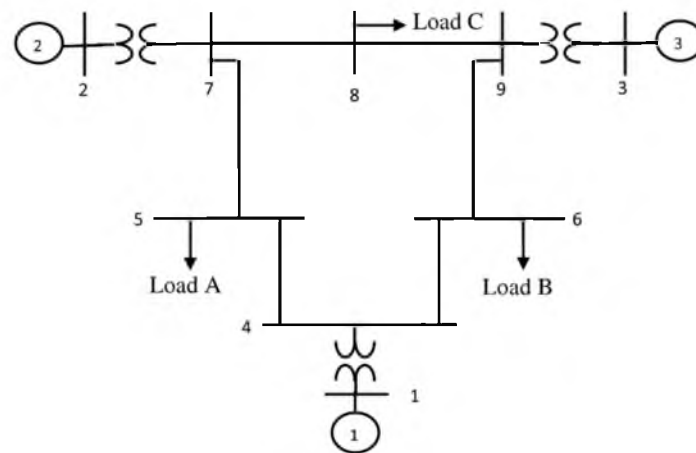

Figure 6. 3-machine, 9-bus power system from WSCC.

Table 8. System operating conditions.

Generator	Normal Case		Case 1		Case 2		Case 3	
	P(p.u)	Q(p.u)	P(p.u)	Q(p.u)	P(p.u)	Q(p.u)	P(p.u)	Q(p.u)
G_1	1.79	0.28	2.11	1.19	0.33	1.12	1.47	1.05
G_2	1.65	0.08	1.22	0.57	2.00	0.57	2.01	0.6
G_3	0.85	−0.11	1.29	0.38	1.50	0.38	1.5	0.7
Load								
A	1.25	0.54	2.10	0.70	1.50	0.90	1.5	0.9
B	0.90	0.31	1.81	0.450	1.20	0.80	1.2	0.8
C	1.10	0.25	1.70	0.80	1.00	0.5	1	0.5

The objective function given in Equation (10) is minimized with two scenarios of severe fault disturbances under the loading conditions described above in order to find the optimum values of controllers' parameters. Scenario 1: The line 5–7 close bus 5 experiences a 6-cycle fault disturbance. The fault is cleared by tripping line 5–7 and reclosing it successfully after 1.0 s. Scenario 2 is the same as scenario 1, except for a 0.2 (pu) step increase in mechanical power. Lines 5–7 are tripped to clear the fault and reclosing successfully after 1.0 s. The optimum controller parameters obtained using the nonlinear time domain based objective function are shown in Table 9. To obtain the results presented in this table, the problem has been solved 30 times using the proposed hCSC-PS and the best results are presented in Table 9. After the proposed hCSC-PS technique had converged, these results were obtained. To demonstrate the robustness of the coordination between PSSs and SVC controllers, an individual design is also carried out.

Table 9. Optimal parameters obtained by hCSC-PS.

Algorithm		K	T_1	T_2	T3	T_4
Uncoordinated design	PSS1	20.45	0.070	0.073	0.030	0.045
	PSS2	19.36	0.128	0.050	0.068	0.055
	SVC	65.56	0.028	0.121	0.523	0.048
Coordinated design	PSS1	24.06	0.095	0.043	0.283	0.050
	PSS2	15.03	0.056	0.050	0.054	0.029
	SVC	25.02	0.028	0.230	0.058	0.493

Figure 7 shows the speed deviation response for various loading conditions under two scenarios to demonstrate the contribution of the coordinated design versus the uncoordinated design. When compared to when no controllers are used, Figure 8 clearly shows that SVC-based controllers fail to provide adequate damping of system oscillations when used alone. Furthermore, when compared to SVC controllers, PSSs regulators provide good damping of system oscillations with a short settling time. The suggested coordinated controllers, on the other hand, remain the most effective at damping oscillations and reducing their settling times. The coordinated design of the suggested method outperforms the uncoordinated design, according to the simulation results.
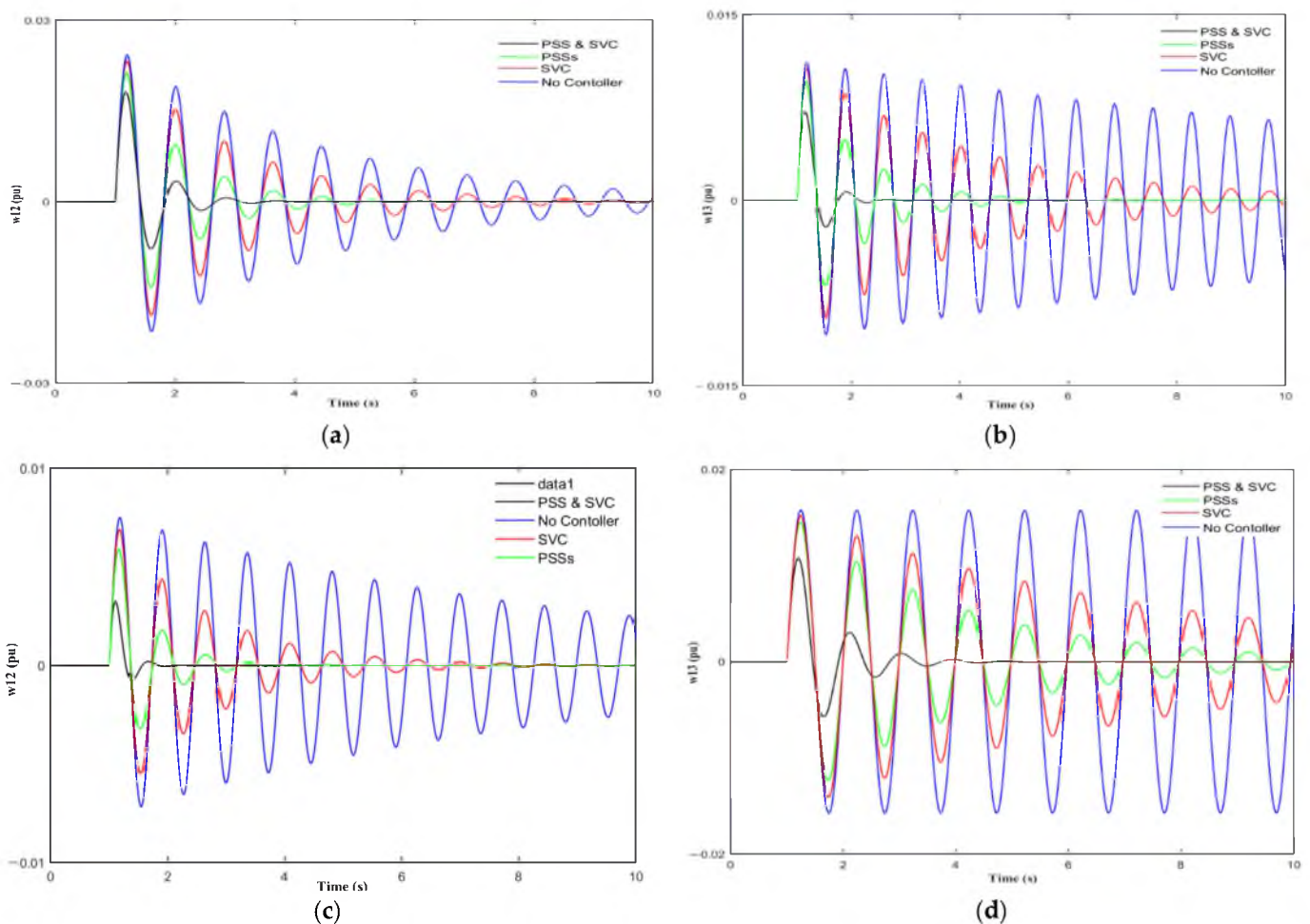

Figure 7. Speed deviation response for various loading conditions. (**a**) Normal case scenario 1; (**b**) Case 1 under scenario 2; (**c**) Case 2 under scenario 1; (**d**) Case 3 under scenario 2.

To determine the robustness of the suggested controllers, the parameters of the controllers are also tuned using SCA, TSA, and GSA methods. The values of these parameters are shown in Table 10. Figure 8 depicts the rate of convergence for the best controller tuning. By minimizing a time domain objective function with speed deviations, the proposed method is used to solve the problem of controller parameter design in a multi-machine power system. In addition, when a controller is designed with HCSC-PS, GSA, TSA, and SCA, over the simulation period, the speed divergence is calculated, as shown in Figure 9. Note that $w_{12} = w_2 - w_1$ and $w_{13} = w_3 - w_1$. The PSS and SVC controllers built by hCSC-PS provide good damping for the study system and have a superior feature than those designed by SCA, GSA, and TSA, as seen in these graphs. Obtained minimum damping ratios are presented in Table 11 for different loading conditions. The higher values of minimum damping ratio depict the higher capability of the controller to damp out the LFOs. As can be seen from Table 11, proposed method give the larger value of minimum damping ratio compared to the other methods. This means that PSS and SVC controllers optimized by hCSC-PS are capable of providing better damping to the LFOs. The damping ratio is a dimensionless parameter which describes how an oscillating comes to rest. The damping ratio describes how rapidly the amplitude of a vibrating system decays with respect to time. By increasing the system damping ratio, the forced oscillation amplitude can be reduced. The damping ratio of the oscillation is defined as:

$$\zeta = \frac{-\sigma}{\sqrt{\sigma^2 + \omega^2}} \tag{12}$$

Table 10. Optimal parameters obtained by SCA, TSA, and GSA.

Algorithm		K	T_1	T_2	T3	T_4
	PSS1	20.30	0.254	0.854	0.221	1.214
Coordinated by SCA	PSS2	17.24	0.052	0.563	0.034	0.376
	SVC	36.92	0.058	0.034	0.031	0.098
	PSS1	18.24	0.021	0.267	0.181	0.276
Coordinated by TSA	PSS2	26.08	0.854	0.189	0.023	1.149
	SVC	18.65	0.523	0.123	0.081	0.100
	PSS1	25.45	0.283	0.854	0.63	1.312
Coordinated by GSA	PSS2	18.05	0.054	0.561	0.101	0.734
	SVC	51.23	0.058	0.034	0.045	0.087

Table 11. Damping ratio comparison for different loading conditions.

	Uncoordinated Design	Coordinated Design	Coordinated by SCA	Coordinated by TSA	Coordinated by GSA
Case 1	0.0696	0.7779	0.5654	0.5412	0.2524
Case 2	0.2868	0.8379	0.5003	0.5177	0.5215
Case 3	0.2139	0.7686	0.4538	0.4417	0.5459
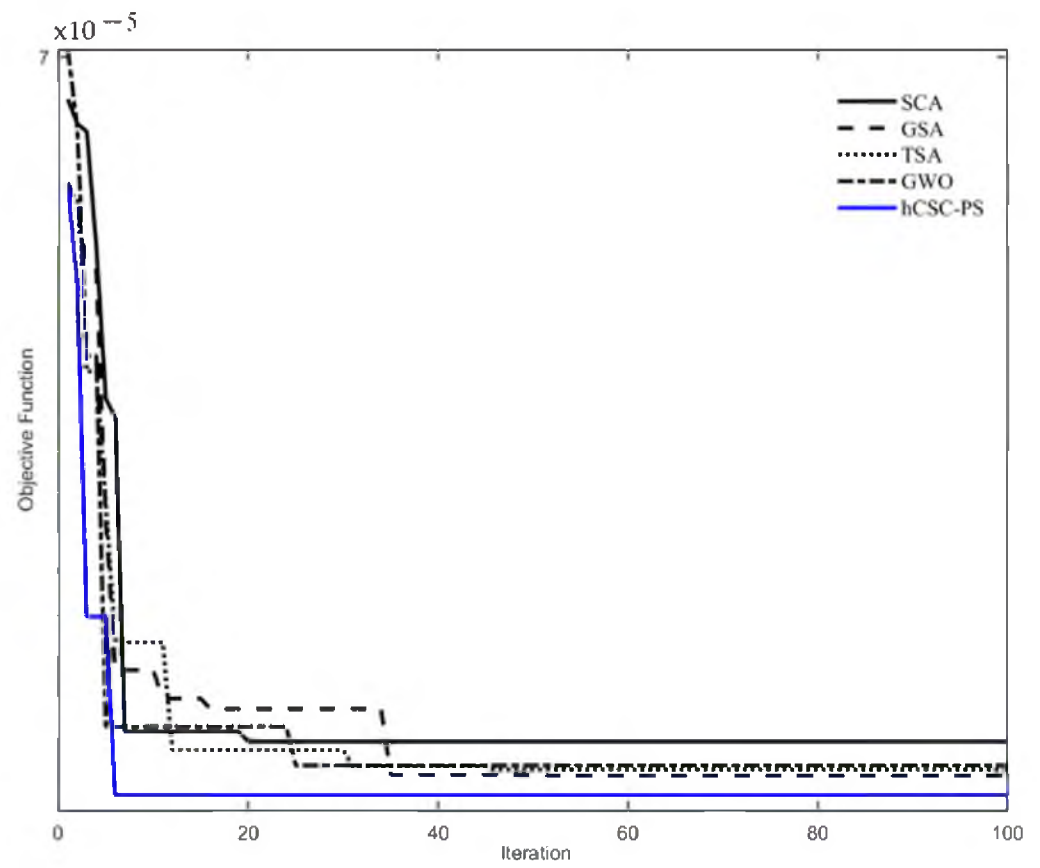
Figure 8. Fitness Convergence with hCSC-PS, GSA, TSA, GWO, SCA.

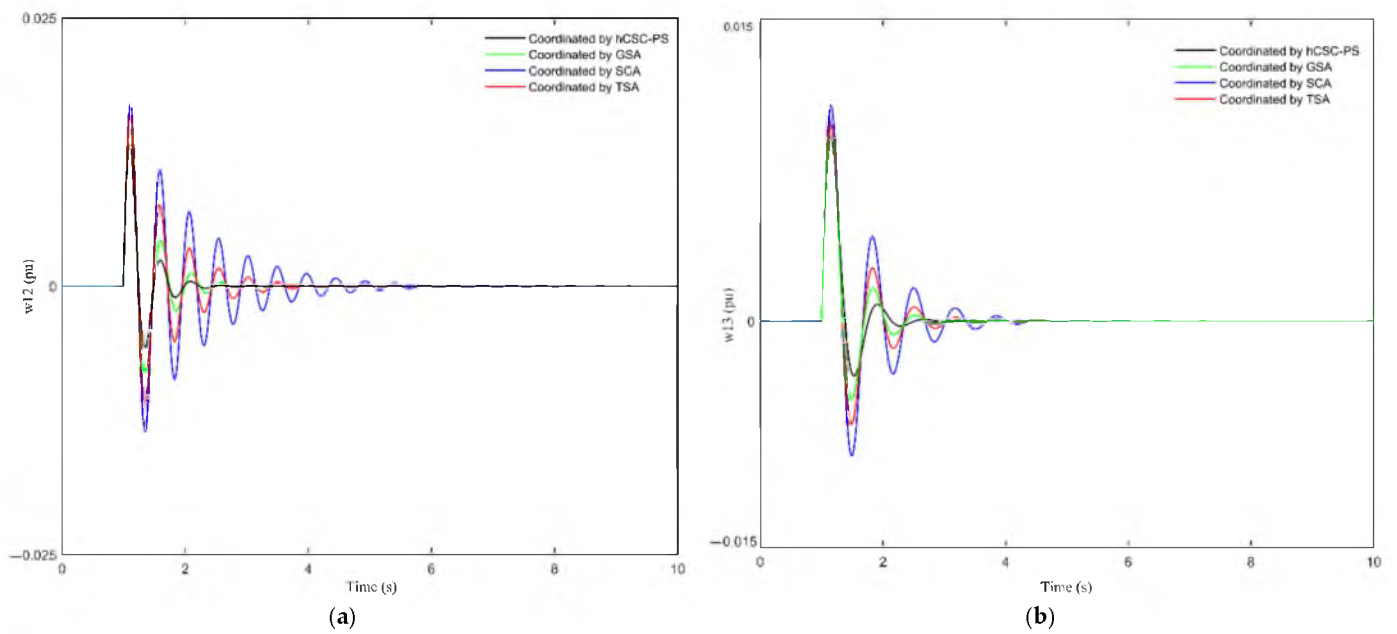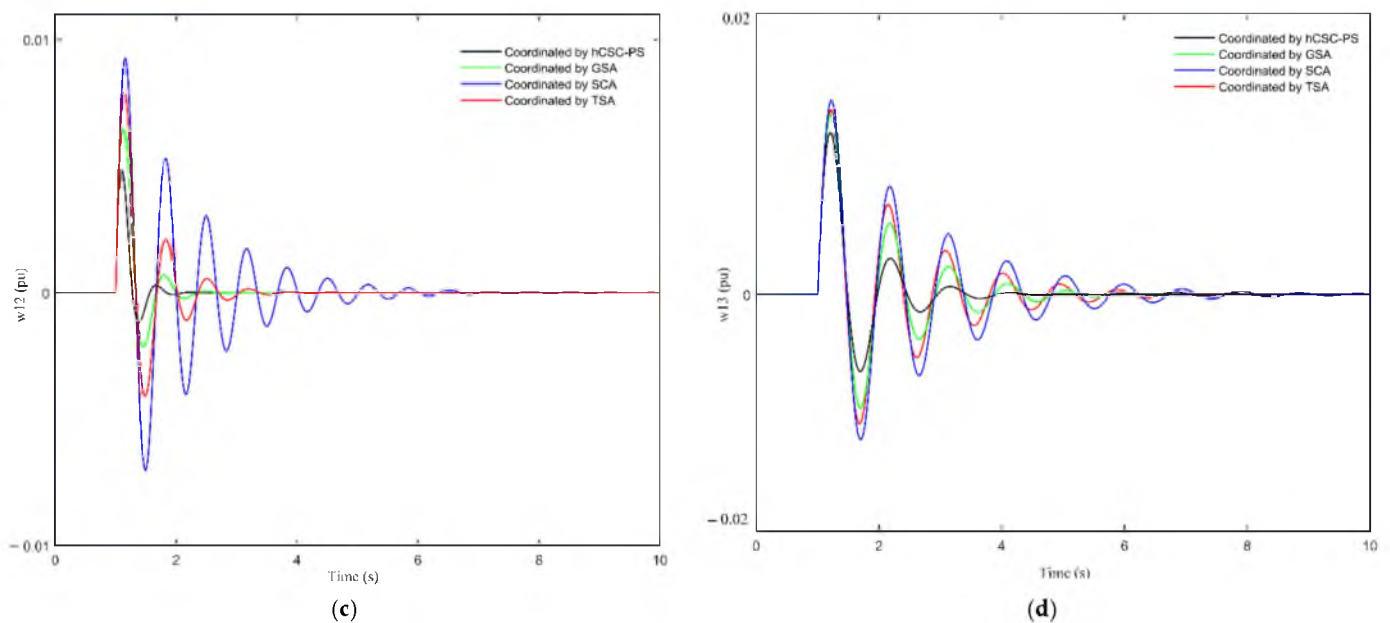**(a)**

(b)

Figure 9. *Cont.*

Figure 9. Speed deviation response for various loading conditions. (**a**) Normal Case under scenario 1; (**b**) Case 1 under scenario 2; (**c**) Case 2 under scenario 1; (**d**) Case 3 under scenario 2.

6. Conclusions

In this paper, a novel hybrid optimization algorithm called hCSC-PS is suggested for the simultaneous coordinated design of PSSs and SVC controllers in multi-machine power system. The proposed hCSC-PS combines two search techniques: the chaotic CSA as an effective global optimization, and pattern search as a robust local search method. Firstly, the performance comparison of the proposed hCSC-PS algorithm on a set of benchmark functions reveals that the proposed method outperforms the standard SCA and also other algorithms. Then, the problem is formulated as an optimization problem where the controllers' parameters are the decision variables of the problem. The enhancement of the system stability is taken into account in the objective function in which the time responses of the speeds' deviations of machines are involved. Then, the hCSC-PS algorithm is used to optimize the objective function for four operating conditions (representative cases) and severe fault scenarios. The performance and robustness of the proposed controller are assessed on a power network test, frequently used in power system stability studies. Simulation results showed that the proposed coordinated design of PSSs and SVC controllers greatly improved the damping characteristics of power system oscillations, compared to the individual design.

Author Contributions: Conceptualization, M.N.; methodology, M.E.; software, M.E.; validation, M.E., M.N. and S.A.K.; formal analysis, M.E. and S.A.K.; investigation, M.N.; resources, M.E.; data curation, M.E. and M.N.; writing—original draft preparation, M.E. and S.A.K.; writing—review and editing, M.E., S.A.K. and M.N.; visualization, M.E.; supervision, M.E.; project administration, M.E.; funding acquisition, M.N. All authors have read and agreed to the published version of the manuscript.

Appendix A

The dynamics model of power system is given by [58]:

Appendix A.1. Generator

$$\dot{\delta}_i = \omega_b(\omega_i - 1) \tag{A1}$$

$$\dot{\omega}_i = \frac{1}{M_i}\left(P_{mi} - P_{ei} - D_i(\omega_i - 1)\right) \tag{A2}$$

$$\dot{E}'_{qi} = \frac{1}{T'_{doi}}\left(E_{fdi} - \left(\dot{x}_{di} - \acute{x}_{di}\right)i_{di} - \acute{E}_{qi}\right) \tag{A3}$$

$$P_{ei} = v_{di}i_{di} + v_{qi}i_{qi} \tag{A4}$$

Appendix A.2. Exciter and PSS

$$\dot{E}'_{fdi} = \frac{1}{T'_{Ai}}\left(K_{Ai}(v_{refi} - v_i + u_{PSSi}) - E_{fdi}\right) \tag{A5}$$

$$v_i = \left(v^2_{di} + v^2_{qi}\right)^{1/2} \tag{A6}$$

$$v_{di} = x_{qi}i_{qi} \tag{A7}$$

$$v_{qi} = \acute{E}_{qi} - \acute{x}_{di}\acute{i}_{di} \tag{A8}$$

$$T_{ei} = \acute{E}_{qi}i_{qi}\left(x_{qi} - \acute{x}_{di}\right)i_{di}i_{qi} \tag{A9}$$

Appendix A.3. SVC- Based Controller

$$\dot{B}_{SVC} = \left(K_s\left(B^{ref}_{SVC} - u_{SVC}\right) - B_{SVC}\right)/T_s \tag{A10}$$

Appendix A.4. Linearized Model

$$\begin{bmatrix} \Delta\dot{\delta} \\ \Delta\dot{\omega} \\ \Delta\dot{E}'_q \\ \Delta\dot{E}_{fd} \end{bmatrix} + \begin{bmatrix} 0 & \omega_0 I & 0 & 0 \\ -M^{-1}K_1 & -M^{-1}D & -M^{-1}K_2 & 0 \\ -T'^{-1}_{do}K_4 & 0 & -T'^{-1}_{do}K_3 & T'^{-1}_{do} \\ -T^{-1}_A K_A K_5 & 0 & -T^{-1}_A K_A K_6 & T^{-1}_A \end{bmatrix} \begin{bmatrix} \Delta\delta \\ \Delta\omega \\ \Delta E'_q \\ \Delta E_{fd} \end{bmatrix}$$
$$+ \begin{bmatrix} 0 & 0 \\ 0 & -M^{-1}K_{pB} \\ 0 & -T'^{-1}_{do}K_{qB} \\ T^{-1}_A K_A & -T^{-1}_A K_A K_{vB} \end{bmatrix} \begin{bmatrix} u_{PSSi} \\ \Delta B \end{bmatrix} \tag{A11}$$

$$K_1 = \frac{\partial P_e}{\partial \delta}, K_2 = \frac{\partial P_e}{\partial E'_q}, K_3 = \frac{\partial E_q}{\partial E_q}, K_4 = \frac{\partial E_q}{\partial \delta}, K_5 = \frac{\partial v}{\partial \delta}, K_6 = \frac{\partial v}{\partial E_q}, K_{pB} = \frac{\partial P_e}{\partial B}, K_{qB} = \frac{\partial v}{\partial E_q}, K_{vB} = \frac{\partial v}{\partial B} \tag{A12}$$

Appendix B

Table A1. Nomenclature and Abbreviation.

Variables & Abbreviation	Description	Variables & Abbreviation	Description
$f(X)$	Fitness function	dim	Dimension
$g(X)$	Inequality constraints	SF	Size factor
$h(X)$	Equality constraints	P_{mi}	Mechanical input power
X	Dimensional vector of design variables	P_{ei}	Active power
X^L & X^U	Boundary constraints	M	Machine inertia
δ	Rotor angle	D	Damping the coefficient
ω	Speed deviation	v_{refi}	Reference voltage
E_q	Internal voltages	T_{doi}	Open circuit field time constant
E_{fa}	Field voltages	i_{di}, i_{qi}	Stator currents in d- and q -axis circuits
u	Input control parameters	x	Vector of state variables
t_{sim}	time of simulation	y	Vector of algebraic variables
N	Number of machines	B_{SVC}	Susceptance of SVC
M	Number of operating points	ξ	Damping ratio
K	Gain	F_{min}	Minimum value of the objective function
T_1–T_4	Time constants	dim	dimension
T_{Wi}	Time constant of washout	A	$4n \times 4n$ matrix
x_i	Placement of ith solution in the search space	B	$4n \times m$ matrix
ub_i	Upper bounds	a	Control parameter
lb_i	Lower bounds	m	*PSS* and *SVC*
r_3	Random number among 0 and 1	X	$4n \times 1$ state vector
x_i^t	Position of ith solution at iteration t	SF	Size factor
x_{Best}	Best solution in the population	PSS	Power system stabilizer
r_1	Random numbers in the range of $[0, 2\pi]$	SVC	Static VAR compensator
r_2	Random weight of the best solution	CSCA	Chaotic sine cosine algorithm
t_{max}	Maximum number of iterations	PS	Pattern search
$\lambda(t)$	Chaotic map	FACTS	Flexible AC transmission systems
t	Iteration number	hCSC-PS	Hybrid CSCA and PS
a	Constant equal to 4	LFO	Low frequency oscillations
W_{12}	Speed difference response of G_1–G_2	SQP	Sequential quadratic programming
W_{13}	Speed difference response of G_1–G_3	SCA	Sine cosine algorithm
K_1–K_6	Linearization constants	K_p, K_q, K_B	Linearization constants

References

1. Kundur, P.; Balu, N.J.; Lauby, M.G. *Power System Stability and Control*; McGraw Hill: New York, NY, USA, 1994; p. 7.
2. Hingorani, N.G. FACTS-flexible AC transmission system. In *International Conference on AC and DC Power Transmission*; IET: London, UK, 1991; pp. 1–7.
3. Eslami, M.; Shareef, H.; Mohamed, A.; Khajehzadeh, M. A Survey on Flexible AC Transmission Systems (FACTS). *Przeglad Elektrotechniczny* **2012**, *88*, 1–11.
4. Chen, J.-H.; Lee, W.-J.; Chen, M.-S. Using a static var compensator to balance a distribution system. In Proceedings of the IAS'96 Conference Record of the 1996 IEEE Industry Applications Conference Thirty-First IAS Annual Meeting, San Diego, CA, USA, 6–10 October 1996; IEEE: Piscataway, NJ, USA, 1996; pp. 2321–2326.
5. Anderson, P.M.; Fouad, A.A. *Power System Control and Stability*; John Wiley & Sons: Hoboken, NJ, USA, 2008.
6. Noroozian, M.; Adersson, G. Damping of power system oscillations by use of controllable components. *IEEE Trans. Power Deliv.* **1994**, *9*, 2046–2054. [CrossRef]
7. Eslami, M.; Shareef, H.; Khajehzadeh, M. Optimal design of damping controllers using a new hybrid artificial bee colony algorithm. *Int. J. Electr. Power Energy Syst.* **2013**, *52*, 42–54. [CrossRef]
8. Khajehzadeh, M.; Taha, M.R.; El-Shafie, A.; Eslami, M. Search for critical failure surface in slope stability analysis by gravitational search algorithm. *Int. J. Phys. Sci.* **2011**, *6*, 5012–5021.
9. Talaat, M.; Hatata, A.; Alsayyari, A.S.; Alblawi, A. A smart load management system based on the grasshopper optimization algorithm using the under-frequency load shedding approach. *Energy* **2020**, *190*, 116423. [CrossRef]
10. Talaat, M.; Farahat, M.; Mansour, N.; Hatata, A. Load forecasting based on grasshopper optimization and a multilayer feed-forward neural network using regressive approach. *Energy* **2020**, *196*, 117087. [CrossRef]
11. Talaat, M.; Said, T.; Essa, M.A.; Hatata, A. Integrated MFFNN-MVO approach for PV solar power forecasting considering thermal effects and environmental conditions. *Int. J. Electr. Power Energy Syst.* **2022**, *135*, 107570. [CrossRef]
12. Rana, M.J.; Shahriar, M.S.; Shafiullah, M. Levenberg–Marquardt neural network to estimate UPFC-coordinated PSS parameters to enhance power system stability. *Neural Comput. Appl.* **2019**, *31*, 1237–1248. [CrossRef]
13. Shafiullah, M.; Abido, M.; Coelho, L. Design of robust PSS in multimachine power systems using backtracking search algorithm. In Proceedings of the 2015 18th International Conference on Intelligent System Application to Power Systems (ISAP), Porto, Portugal, 11–16 September 2015; IEEE: Piscataway, NJ, USA, 2015; pp. 1–6.
14. Firouz, M.H.; Ghadimi, N. Concordant controllers based on FACTS and FPSS for solving wide-area in multi-machine power system. *J. Intell. Fuzzy Syst.* **2016**, *30*, 845–859. [CrossRef]
15. Farah, A.; Guesmi, T.; Abdallah, H.H.; Ouali, A. A novel chaotic teaching–learning-based optimization algorithm for multi-machine power system stabilizers design problem. *Int. J. Electr. Power Energy Syst.* **2016**, *77*, 197–209. [CrossRef]
16. Abd-Elazim, S.; Ali, E. Coordinated design of PSSs and SVC via bacteria foraging optimization algorithm in a multimachine power system. *Int. J. Electr. Power Energy Syst.* **2012**, *41*, 44–53. [CrossRef]
17. Choudhury, S.; Dash, T. Modified brain storming optimization technique for transient stability improvement of SVC controller for a two machine system. *World J. Eng.* **2021**, *18*, 841–850. [CrossRef]
18. Guesmi, T.; Alshammari, B.M.; Almalaq, Y.; Alateeq, A.; Alqunun, K. New Coordinated Tuning of SVC and PSSs in Multimachine Power System Using Coyote Optimization Algorithm. *Sustainability* **2021**, *13*, 3131. [CrossRef]
19. Kamarposhti, M.A.; Colak, I.; Iwendi, C.; Band, S.S.; Ibeke, E. Optimal Coordination of PSS and SSSC Controllers in Power System Using Ant Colony Optimization Algorithm. *J. Circuits Syst. Comput.* **2021**, 2250060. [CrossRef]
20. Baadji, B.; Bentarzi, H.; Bakdi, A. Comprehensive learning bat algorithm for optimal coordinated tuning of power system stabilizers and static VAR compensator in power systems. *Eng. Optim.* **2020**, *52*, 1761–1779. [CrossRef]
21. Abido, M.; Abdel-Magid, Y. Coordinated design of a PSS and an SVC-based controller to enhance power system stability. *Int. J. Electr. Power Energy Syst.* **2003**, *25*, 695–704. [CrossRef]
22. Kamari, N.A.M.; Musirin, I.; Ibrahim, A.A. Swarm intelligence approach for angle stability improvement of PSS and SVC-based SMIB. *J. Electr. Eng. Technol.* **2020**, *15*, 1001–1014. [CrossRef]
23. Abdelaziz, A.Y.; Ali, E.S. Static VAR compensator damping controller design based on flower pollination algorithm for a multi-machine power system. *Electr. Power Compon. Syst.* **2015**, *43*, 1268–1277. [CrossRef]
24. Eslami, M.; Shareef, H.; Mohamed, A.; Khajehzadeh, M. PSS and TCSC damping controller coordinated design using GSA. *Energy Procedia* **2012**, *14*, 763–769. [CrossRef]
25. Eslami, M.; Shareef, H.; Mohamed, A.; Khajehzadeh, M. Gravitational search algorithm for coordinated design of PSS and TCSC as damping controller. *J. Cent. South Univ.* **2012**, *19*, 923–932. [CrossRef]
26. Kar, M.K.; Kumar, S.; Singh, A.K.; Panigrahi, S. A modified sine cosine algorithm with ensemble search agent updating schemes for small signal stability analysis. *Int. Trans. Electr. Energy Syst.* **2021**, *31*, e13058. [CrossRef]
27. Bhukya, J.; Naidu, T.A.; Vuddanti, S.; Konstantinou, C. Coordinated control and parameters optimization for PSS, POD and SVC to enhance the transient stability with the integration of DFIG based wind power systems. *Int. J. Emerg. Electr. Power Syst.* **2021**. [CrossRef]
28. Pandey, R.K.; Gupta, D.K. Performance evaluation of power oscillation damping controller—Firefly algorithm based parameter tuning. *Electr. Power Compon. Syst.* **2017**, *45*, 2164–2174. [CrossRef]

29. Panda, S. Robust coordinated design of multiple and multi-type damping controller using differential evolution algorithm. *Int. J. Electr. Power Energy Syst.* **2011**, *33*, 1018–1030. [CrossRef]

30. Karthikeyan, K.; Lakshmi, P. Optimal design of PID controller for improving rotor angle stability using BBO. *Procedia Eng.* **2012**, *38*, 889–902. [CrossRef]

31. Abd Elazim, S.; Ali, E. Optimal power system stabilizers design via cuckoo search algorithm. *Int. J. Electr. Power Energy Syst.* **2016**, *75*, 99–107. [CrossRef]

32. Naresh, G.; Raju, M.R.; Narasimham, S. Coordinated design of power system stabilizers and TCSC employing improved harmony search algorithm. *Swarm Evol. Comput.* **2016**, *27*, 169–179. [CrossRef]

33. Afzalan, E.; Joorabian, M. Analysis of the simultaneous coordinated design of STATCOM-based damping stabilizers and PSS in a multi-machine power system using the seeker optimization algorithm. *Int. J. Electr. Power Energy Syst.* **2013**, *53*, 1003–1017. [CrossRef]

34. Bijami, E.; Marnani, J.A. Imperialist Competitive Algorithm for Optimal Simultaneous Coordinated Tuning of Damping Controller. *Int. J. Tech. Phys. Probl. Eng. (IJTPE)* **2012**, *11*, 34–41.

35. Devarapalli, R.; Bhattacharyya, B. Application of modified harris hawks optimization in power system oscillations damping controller design. In Proceedings of the 2019 8th International Conference on Power Systems (ICPS), Jaipur, India, 20–22 December 2019; IEEE: Piscataway, NJ, USA, 2019; pp. 1–6.

36. Eslami, M.; Babaei, B.; Shareef, H.; Khajehzadeh, M.; Arandian, B. Optimum Design of Damping Controllers using modified Sperm Swarm Optimization. *IEEE Access* **2021**, *9*, 145592–145604.

37. Abido, M.; Abdel-Magid, Y. A tabu search based approach to power system stability enhancement via excitation and static phase shifter control. *Electr. Power Syst. Res.* **1999**, *52*, 133–143. [CrossRef]

38. Abido, M. Simulated annealing based approach to PSS and FACTS based stabilizer tuning. *Int. J. Electr. Power Energy Syst.* **2000**, *22*, 247–258. [CrossRef]

39. Dhal, P. *Multi-verse Optimizer for Dynamic Stability Analysis Using STATCOM and Power System Stabilizer. Advanced Computing and Intelligent Engineering: Proceedings of ICACIE 2018*; Springer Nature Singapore Pte Ltd.: Singapore, 2020; Volume 2, p. 117.

40. Devarapalli, R.; Bhattacharyya, B.; Kumar, V.; Kumar, S. Improved Moth Flame Optimization in Systematization of STATCOM and PSS. In *Smart Grid Automation and Industry 4.0. Lecture Notes in Electrical Engineering*; Springer: Singapore, 2021; Volume 693, pp. 481–491. [CrossRef]

41. Aribowo, W.; Muslim, S.; Suprianto, B.; Haryudo, S.I. Tunicate Swarm Algorithm-Neural Network for Adaptive Power System Stabilizer Parameter. *Sci. Technol. Asia* **2021**, *26*, 50–63.

42. Dey, P.; Bhattacharya, A.; Das, P. Tuning of power system stabilizer for small signal stability improvement of interconnected power system. *Appl. Comput. Inform.* **2017**, *16*, 3–28. [CrossRef]

43. Asghari, K.; Masdari, M.; Gharehchopogh, F.S.; Saneifard, R. Multi-swarm and chaotic whale-particle swarm optimization algorithm with a selection method based on roulette wheel. *Expert Syst.* **2021**, *38*, e12779. [CrossRef]

44. Farah, A.; Belazi, A.; Alqunun, K.; Almalaq, A.; Alshammari, B.M.; Ben Hamida, M.B.; Abbassi, R. A New Design Method for Optimal Parameters Setting of PSSs and SVC Damping Controllers to Alleviate Power System Stability Problem. *Energies* **2021**, *14*, 7312. [CrossRef]

45. Sahu, P.R.; Hota, P.K.; Panda, S. Modified whale optimization algorithm for coordinated design of fuzzy lead-lag structure-based SSSC controller and power system stabilizer. *Int. Trans. Electr. Energy Syst.* **2019**, *29*, e2797. [CrossRef]

46. Eslami, M.; Shareef, H.; Mohamed, A.; Khajehzadeh, M. Optimal location of PSS using improved PSO with chaotic sequence. In Proceedings of the International Conference on Electrical, Control and Computer Engineering 2011 (InECCE), Kuantan, Malaysia, 21–22 June 2011; IEEE: Piscataway, NJ, USA, 2011; pp. 253–258.

47. Khajehzadeh, M.; Taha, M.R.; Eslami, M. A new hybrid firefly algorithm for foundation optimization. *Natl. Acad. Sci. Lett.* **2013**, *36*, 279–288. [CrossRef]

48. Eslami, M.; Shareef, H.; Mohamed, A. Optimization and coordination of damping controls for optimal oscillations damping in multi-machine power system. *Int. Rev. Electr. Eng.* **2011**, *6*, 1984–1993.

49. Mirjalili, S. SCA: A sine cosine algorithm for solving optimization problems. *Knowl.-Based Syst.* **2016**, *96*, 120–133. [CrossRef]

50. Abualigah, L.; Diabat, A. Advances in sine cosine algorithm: A comprehensive survey. *Artif. Intell. Rev.* **2021**, *54*, 2567–2608. [CrossRef]

51. Ji, Y.; Tu, J.; Zhou, H.; Gui, W.; Liang, G.; Chen, H.; Wang, M. An adaptive chaotic sine cosine algorithm for constrained and unconstrained optimization. *Complexity* **2020**, *2020*, 6084917. [CrossRef]

52. Wolpert, D.H.; Macready, W.G. No free lunch theorems for optimization. *IEEE Trans. Evol. Comput.* **1997**, *1*, 67–82. [CrossRef]

53. Torczon, V. On the convergence of pattern search algorithms. *SIAM J. Optim.* **1997**, *7*, 1–25. [CrossRef]

54. Rashedi, E.; Nezamabadi-Pour, H.; Saryazdi, S. GSA: A gravitational search algorithm. *Inf. Sci.* **2009**, *179*, 2232–2248. [CrossRef]

55. Kaur, S.; Awasthi, L.K.; Sangal, A.; Dhiman, G. Tunicate swarm algorithm: A new bio-inspired based metaheuristic paradigm for global optimization. *Eng. Appl. Artif. Intell.* **2020**, *90*, 103541. [CrossRef]

56. Mirjalili, S.; Mirjalili, S.M.; Lewis, A. Grey wolf optimizer. *Adv. Eng. Softw.* **2014**, *69*, 46–61. [CrossRef]

57. Pai, M.; Gupta, D.S.; Padiyar, K. *Small Signal Analysis of Power Systems*; Alpha Science Int'l Ltd.: Oxford, UK, 2004.

58. Sadikovic, R.; Andersson, G.; Korba, P. Damping controller design for power system oscillations. *Intell. Autom. Soft Comput.* **2006**, *12*, 51–62. [CrossRef]